J|A|C|S ARTICLES

Published on Web 08/28/2009

Modification of Symmetrically Substituted Phthalocyanines Using Click Chemistry: Phthalocyanine Nanostructures by Nanoimprint Lithography

Xiaochun Chen,[†] Jayan Thomas,[‡] Palash Gangopadhyay,[‡] Robert A. Norwood,[‡] N. Peyghambarian,[‡] and Dominic V. McGrath*,[†]

Department of Chemistry and College of Optical Sciences, The University of Arizona, Tucson, Arizona 85721

Received July 9, 2009; E-mail: mcgrath@u.arizona.edu

Abstract: Phthalocyanines (Pcs) are commonly applied to advanced technologies such as optical limiting, photodynamic therapy (PDT), organic field-effect transistors (OFETs), and organic photovoltaic (OPV) devices, where they are used as the p-type layer. An approach to *Pc* structural diversity and the incorporation of a functional group that allows fabrication of solvent resistant *Pc* nanostructures formed by using a newly developed nanoimprint by melt processing (NIMP) technique, a variant of standard nanoimprint lithography (NIL), is reported. Copper(I)-catalyzed azide−alkyne cycloaddition (CuAAC), a click chemistry reaction, serves as an approach to structural diversity in *Pc* macrocycles. We have prepared octaalkynyl *Pc* **1b** and have modified this *Pc* using the CuAAC reaction to yield four *Pc* derivatives **5a**−**5d** with different peripheral substituents on the macrocycle. One of these derivatives, **5c**, has photo-cross-linkable cinnamate residues, and we have demonstrated the fabrication of robust cross-linked photopatterned and imprinted nanostructures from this material.

Introduction

Phthalocyanines (Pcs) are commonly applied to advanced technologies such as optical limiting,[1] photodynamic therapy (PDT),[2] organic field-effect transistors (OFETs),[3] and organic photovoltaic (OPV) devices,[4−6] where they are used as the p-type layer. Critical to the performance of *Pc* materials in these applications is the condensed phase morphology that they adopt and the nanostructures into which they can be fabricated. *Pc* solid state properties including self-association and interfacial behavior are dependent on substituents on the periphery of the chromophore.[7] Extremely subtle structural variations in disk-like chromophores can lead to dramatic and effective alteration of their condensed phase organization, with a resultant effect on the electronic interactions between adjacent molecules.[8] To study the influence of *Pc* structure on condensed phase morphology, a library of different Pcs must be created to survey the effects of structural alterations. However, while the extent of structural variation of *Pc* materials to date is quite impressive,[9] there is a need for general methods of producing *Pc* materials with structural diversity, especially with substituents that will not readily survive the relatively harsh conditions of *Pc* chromophore synthesis.[10]

Here we disclose an approach to *Pc* structural diversity based on "click chemistry".[11] We have chosen the copper(I)-catalyzed azide−alkyne cycloaddition (CuAAC)[12] as an approach to structural diversity in *Pc* macrocycles. A click chemistry reaction, CuAAC has proven useful for the synthesis of novel polymers and materials in many laboratories[13] and is an ideal

[†] Department of Chemistry.
[‡] College of Optical Sciences.

(1) (a) Dini, D.; Barthel, M.; Hanack, M. *Eur. J. Org. Chem.* **2001**, 3759–3769. (b) O'Flaherty, S. M.; Hold, S. V.; Cook, M. J.; Torres, T.; Chen, Y.; Hanack, M.; Blau, W. J. *Adv. Mater.* **2003**, *15*, 19–32. (c) Chen, Y.; Hanack, M.; Araki, Y.; Ito, O. *Chem. Soc. Rev.* **2005**, *34*, 517. (d) de la Torre, G.; Vazquez, P.; Agullo-Lopez, F.; Torres, T. *Chem. Rev.* **2004**, *104*, 3723.
(2) (a) Bonnett, R. *Chem. Soc. Rev.* **1995**, *24*, 19–33. (b) Pandey, R. K.; Zheng, G. *Porphyrin Handbook* **2000**, *6*, 157–230. (c) Moreira, L. M.; dos Santos, F. V.; Lyon, J. P.; Maftoum-Costa, M.; Pacheco-Soares, C.; da Silva, N. S. *Aust. J. Chem.* **2008**, *61*, 741–754.
(3) Bouvet, M. *Anal. Bioanal. Chem.* **2006**, *384*, 366–373.
(4) Shaheen, S. E.; Ginley, D. S.; Jabbour, G. E. *MRS Bull.* **2005**, *30*, 10–19.
(5) (a) Yoo, S.-Y.; Domercq, B.; Donley, C. L.; Carter, C.; Xia, W.; Minch, B. A.; O'Brien, D. F.; Armstrong, N. R.; Kippelen, B. *SPIE: Organic Photovoltaics IV* **2004**, *5215*, 71–78. (b) Brumbach, M.; Placencia, D.; Armstrong, N. R. *J. Phys. Chem. C* **2008**, *112*, 3142.
(6) (a) Xue, J.; Rand, B. P.; Uchida, S.; Forrest, S. R. *J. Appl. Phys.* **2005**, *98*, 124903. (b) Xue, J.; Rand, B. P.; Uchida, S.; Forrest, S. R. *Adv. Mater.* **2005**, *17*, 66–71. (c) Thompson, B. C.; Fréchet, J. M. J. *Angew. Chem., Int. Ed.* **2008**, *47*, 58–77. (d) Ma, W.; Yang, C.; Gong, X.; Lee, K.; Heeger, A. J. *Adv. Funct. Mater.* **2005**, *15*, 1617–1622. (e) Li, G.; Shrotriya, V.; Huang, J.; Yao, Y.; Moriarty, T.; Emery, K.; Yang, Y. *Nat. Mater.* **2005**, *4*, 864–868. (f) Reyes-Reyes, M.; Kim, K.; Carroll, D. L. *Appl. Phys. Lett.* **2005**, *87*, 083506. (g) Xue, J. G.; Uchida, S.; Rand, B. P.; Forrest, S. R. *Appl. Phys. Lett.* **2004**, *84*, 3013–3015.
(7) Elemans, J. A. A. W.; van Hameren, R.; Nolte, R. J. M.; Rowan, A. E. *Adv. Mater.* **2006**, *18*, 1251–1266.
(8) Huijser, A.; Savenije, T. J.; Kotlewski, A.; Picken, S. J.; Siebbeles, L. D. A. *Adv. Mater.* **2006**, *18*, 2234+.
(9) de la Torre, G.; Claessens, C. G.; Torres, T. *Chem. Commun.* **2007**, 2000–2015.
(10) de la Torre, G.; Claessens, C. G.; Torres, T. *Eur. J. Org. Chem.* **2000**, 2821–2830.
(11) Kolb, H. C.; Finn, M. G.; Sharpless, K. B. *Angew. Chem., Int. Ed.* **2001**, *40*, 2004–2021.
(12) (a) Rostovtsev, V. V.; Green, L. G.; Fokin, V. V.; Sharpless, K. B. *Angew. Chem., Int. Ed.* **2002**, *41*, 2596–2599. (b) Tornoe, C. W.; Christensen, C.; Meldal, M. *J. Org. Chem.* **2002**, *67*, 3057–3064.
(13) Meldal, M.; Tornøe, C. W. *Chem. Rev.* **2008**, *108*, 2952.

10.1021/ja905683g CCC: $40.75

reaction for *Pc* modification due to its extremely high yields and fidelity.[14,15] Incorporation of alkyne functionalities on the periphery of a *Pc* will facilitate alkyne-azide click chemistry, allowing for a variety of high-functioning substituents to be used. With this approach, a library of Pcs can be prepared from a single *Pc* core. Modifying the *Pc* after the macrocycle has been formed eliminates repeating the difficult, low-yielding cyclization step with every desired change in structure. We also demonstrate herein the incorporation of a functional group that allows fabrication of solvent resistant *Pc* nanostructures, formed by using a newly developed nanoimprint by melt processing (NIMP) technique, a variant of standard nanoimprint lithography (NIL).[16]

Results and Discussion

***Pc* Modification by Click Chemistry.** In designing a target for a "clickable" *Pc*, it was necessary to incorporate multiple terminal alkyne moieties on the *Pc* periphery while maintaining good solubility in the typical organic solvents used for click chemistry (e.g., DCM, THF, DMSO). We also sought to minimize the synthetic steps needed to prepare the phthalonitrile precursor to the *Pc*. The ready availability of dihydroxyphthalonitrile **2**[17] and the facile access to alkylated derivatives using Williamson ether or Mitsunobu chemistry[18] led us to posit octaalkynyl **1b** for our clickable *Pc*. In addition to the requisite alkynyl moieties, the four methylene groups between each alkyne moiety and the *Pc* ring would lend degrees of freedom to the structure that may translate to good solubility.

We prepared octaalkynyl *Pc* **1b** via phthalonitrile **4a** or **4b**, both of which were prepared from dihydroxy phthalonitrile **2**[17] by Mitsunobu coupling with either **3a**[19] or commercially available **3b**, respectively (Scheme 1). Linstead cyclization of phthalonitrile **4a** yielded TIPS-protected *Pc* **1a** which was subsequently fluoride-deprotected to provide target **1b** (26% from **4a**). The TIPS groups were initially used to provide a soluble precursor to the potentially poorly soluble **1b**. However, we discovered to our delight that **1b** is *readily soluble in a wide range of organic solvents* (e.g., CH_2Cl_2, $CHCl_3$, THF, acetone, EtOAc). Hence, **1b** is also readily obtained by direct cyclization of phthalonitrile **4b** in 68% yield (Scheme 1). Both **1a** and **1b** were successfully characterized by NMR, UV−vis spectroscopy, mass spectrometry, and combustion analysis. The UV absorption spectrum of both **1a** and **1b** (ca. 10 μM in CH_2Cl_2) were consistent with reported spectra of nonaggregated Pcs[20] with a split Q-band at 702 and 668 nm, vibrational bands at 640 and 607 nm, and B-band at ca. 340 nm (Figure 1a). The GPC traces of both **1a** and **1b** were indicative of monodisperse materials,

Scheme 1

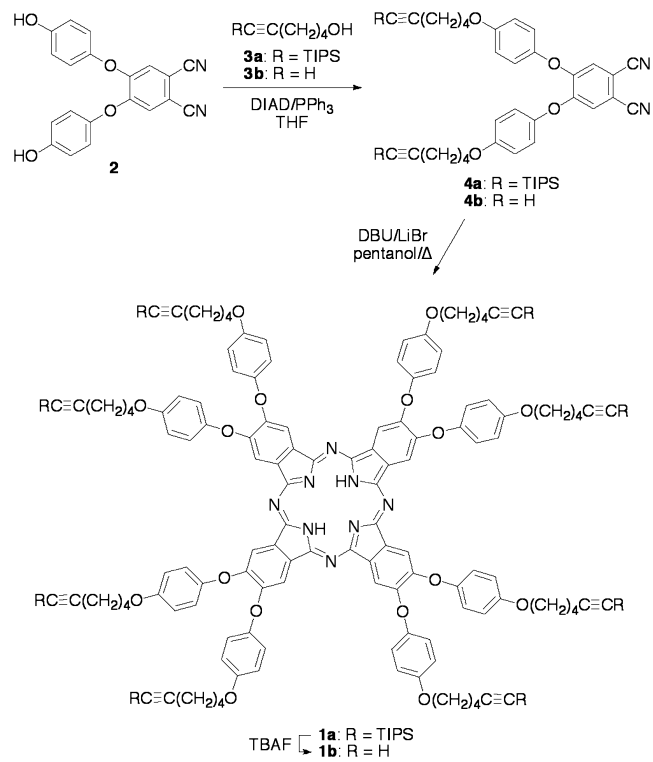

and the hydrodynamic size of TIPs-protected **1a** was larger than that of its deprotected analogue **1b** (Figure 1b).

Octaalkynyl **1b** is an effective platform for *Pc* chromophore modification through click chemistry (Scheme 2). Among click conditions surveyed, a combination of $CuBr(PPh_3)_3$ and Hunig's base in CH_2Cl_2 proved most effective. Using a ratio of 2 azide to 1 alkyne equivalents under these conditions, a reaction time at ambient temperature of 7 days was sufficient to provide octatriazenyl Pcs **5a**−**d** in high yield from **1b** and azides **6a**−**d**. A greater than stoichiometric amount of $CuBr(PPh_3)_3$ was necessary as the metalated CuPcs were obtained under these conditions. We expect that metalation of **1b** prior to click chemistry will allow the use of catalytic amounts of Cu in the preparation of *Pc* with other metal centers.[14] Pcs **5a**−**d** were characterized by a combination of NMR, UV−vis spectroscopy,

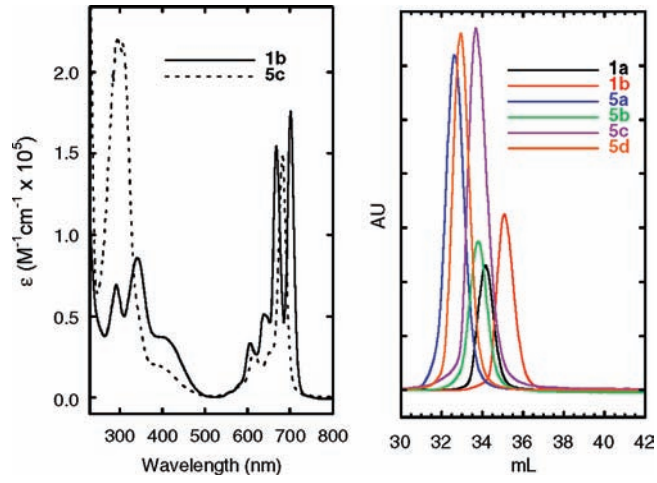

Figure 1. (Left) UV absorption spectra of Pcs **1b** (4.85×10^{-6} M) and **5c** (5.16×10^{-6} M) in DCM. (Right) GPC chromatograms of Pcs **1a**, **1b**, and **5a**−**5d** in THF.

(14) During the preparation of this manuscript, an analogous approach to Pc modification was reported: Jurícek, M.; Kouwer, P. H. J.; Rehák, J.; Sly, J.; Rowan, A. E. *J. Org. Chem.* **2009**, *74*, 21–25.
(15) (a) Campidelli, S.; Ballesteros, B.; Filoramo, A.; Diaz, D.; de la Torre, G.; Torres, T.; Rahman, G. M. A.; Ehli, C.; Kiessling, D.; Werner, F.; Sgobba, V.; Guldi, D. M.; Cioffi, C.; Prato, M.; Bourgoin, J.-P. *J. Am. Chem. Soc.* **2008**, *130*, 11503–11509. (b) Yoshiyama, H.; Shibata, N.; Sato, T.; Nakamura, S.; Toru, T. *Org. Biomol. Chem.* **2008**, *6*, 4498–4501.
(16) Rogers, J. A.; Lee, H. H. *Unconventional Nanopatterning Techniques and Applications*; Wiley: NJ, 2009.
(17) Wöhrle, D.; Eskes, M.; Shigehara, K.; Yamada, A. *Synthesis* **1993**, 194–196.
(18) (a) Kernag, C. A.; McGrath, D. V. *Chem. Commun.* **2003**, 1048–1049. (b) Kernag, C. A.; McGrath, D. V. *Israel J. Chem.* **2009**, *49*, 9–21.
(19) Crimmins, M. T.; Zhang, Y.; Diaz, F. A. *Org. Lett.* **2006**, *8*, 2369–2372.
(20) Brewis, M.; Clarkson, G. J.; Humberstone, P.; Makhseed, S.; McKeown, N. B. *Chem.—Eur. J.* **1998**, *4*, 1633–1640.

Scheme 2

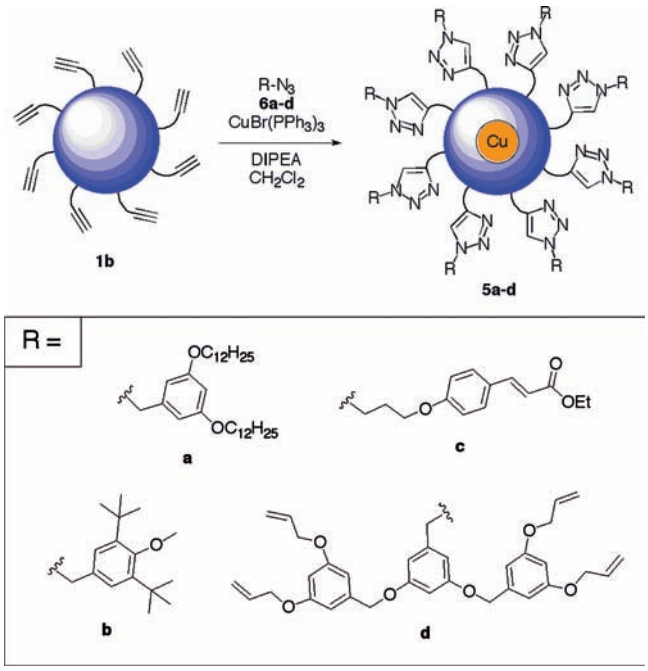

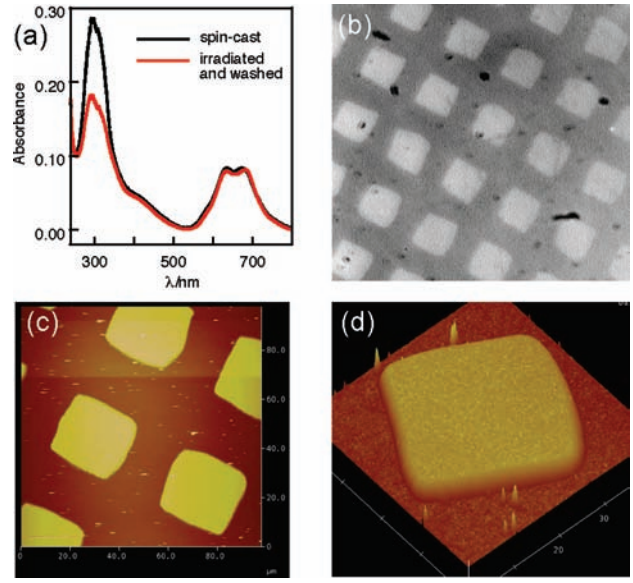

Figure 2. (a) UV absorption spectra of a spin-cast film of **5c** before and after irradiation and wet development. (b) Fluorescence microscopy image of patterned, cross-linked thin films of *Pc* **5c** (495 ± 10 nm excitation and 620 ± 90 nm emission filter). (c and d) AFM image (full images in Supporting Information) of patterned *Pc* **5c** showing 30 μm square features in a 50 nm thin-film.

mass spectrometry, and GPC. The absorption spectra of **5a**−**5d** confirmed the presence of the Cu in the macrocycles, evidenced by the collapsed Q-band resonance at 682 nm (Figure 1a, Supporting Information). The GPC traces of **5a**−**5b** were indicative of monodisperse materials, and the hydrodynamic sizes of all derivatives were larger than those of the corresponding starting material **1b** (Figure 1b).

Micropatterning and Nanofabrication. This method of chromophore modification allows the installation of functional moieties for further manipulation. We demonstrate here both the photopatterning of thin films and imprinting of robust nanostructures using the photo-cross-linking of the cinnamate residues installed onto *Pc* **5c** by click chemistry. Nanostructures of Pcs are of importance for advanced technology applications such as OFETs and OPVs. The control of nanostructure dimension is critical to surmounting the exciton bottleneck problem in heterojunction-based OPVs.[21] To date, OPVs have only reached a maximum power conversion efficiency of ~5%.[6] With a target efficiency of 15−20%,[4] both materials and device design need to be dramatically improved. An increase in efficiency is expected as feature sizes decrease to approach the exciton diffusion length. In addition, exciton mobility is dramatically affected by chromophore organization.[8] The rapid method of chromophore modification described above will allow us to explore both of these aspects of OPV device design. The feature sizes of the nanostructures presented herein approach the exciton diffusion length for OPVs (ca. 20 nm[22]).

To first demonstrate the effectiveness of cross-linking the cinnamate residues on **5c** for producing robust condensed structures, we prepared thin films (ca. 50 nm by ellipsometry) of **5c** by spin-casting from ca. 10^{-6} M CH_2Cl_2 solutions onto quartz. The conditions necessary for successful cross-linking of these films were investigated by subjecting them to irradiation (λ = 310 nm, 6 nm slits) using a 75 W Xe arc lamp. The solid state [2 + 2] photodimerization of the cinnamate residues was easily monitored by changes in the UV absorbance.[23] Continuous irradiation resulted in a decrease in the cinnamate peak in the UV for **5c** (37% overall decrease at 295 nm, λ_{max}) after 95 min (Figure 2a). The decrease in cinnamate absorbance is most likely due to *both* $E \rightarrow Z$ isomerization and [2 + 2] photodimerization. Subsequent wet development (CH_2Cl_2 for 3 min) resulted in negligible change in absorbance for the film of **5c**, indicating the formation of an insoluble cross-linked network (Figure 2a).

Using the conditions for effective cross-linking determined above, we next produced features from these thin films with pattern sizes in the 30 μm range and characterized them by fluorescence microscopy and AFM. Films with ca. 30 μm feature sizes were produced by irradiation (310 nm for 150 min) of a film masked with a transmission electron microscopy (TEM) copper grid (500 mesh) and subsequent wet development in CH_2Cl_2. Patterns of **5c** visualized under a fluorescence microscope (495 ± 10 nm excitation; 620 ± 90 nm emission filter) exhibited resolved features with sharp edges (see Supporting Information). These positive tone images have dark areas with no emissive material and light areas of patterned **5c** with the dimensions of the pattern of the copper grid pattern used as a mask. AFM images (Figure 2b) of the patterned thin film confirmed the feature dimensions (30 μm × 30 μm) as well as the thickness (ca. 50 nm). The similar thickness of the films before and after cross-linking and wet development is evidence of complete polymerization of the pendant cinnamate residues.

Significantly smaller feature sizes were effected in the surface of a thin film of **5c** using a simple but highly efficient technique (NIMP) developed to create nanoarchitectures (Figure 3a). The fundamental difference between NIMP and conventional nanimprinting lithography (NIL) processes is that NIMP starts from a melted material, whereas NIL starts with a spin coated film.

(21) Forrest, S. R. *MRS Bull.* **2005**, *30*, 28–32.
(22) Günes, S.; Neugebauer, H.; Sariciftci, N. S. *Chem. Rev.* **2007**, *107*, 1324.
(23) Bernstein, H. I.; Quimby, W. C. *J. Am. Chem. Soc.* **1943**, *65*, 1845–1846.

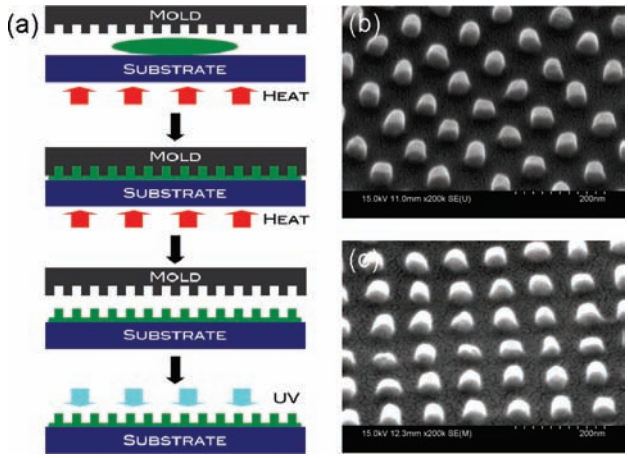

Figure 3. (a) Schematic of the NIMP process. (b) SEM image of a 0.6 μm $\times$ 0.4 μm area of pillars (diameter 40 nm and height 80−100 nm) of **5c** created by NIMP. (c) SEM image of a similar area of pillars after photo-cross-linking.

In NIL, a spin-coated film of a high molecular weight polymer is used as the printing medium. This film is heated to in general 60−100 °C above the glass transition temperature (T_g) of the polymer, and the highly viscous polymer is shaped by pressing the hard mold into it under high pressure. The mold is removed once the polymer is cooled below its glass transition temperature. In NIMP, by contrast, a relatively low molecular weight material is melted on the substrate with no prefabrication of a thin film. Hence, the required pressure for the imprinting process is much lower (about an order of magnitude) in NIMP compared to NIL since the viscosity of the melt is much lower. Due to the low viscosity and small wetting angle of a completely melted material on a silicon (mold) surface, highly efficient nanopatterns can be readily imprinted by the NIMP process. An added advantage of NIMP over NIL is that material loss can be minimized if the required amount of the sample and the thickness are optimized. We have found NIMP to be extremely reliable in printing versatile nanostructures not only for solar cells but also for nanoelectronic and nanophotonic devices, as the technique enables nanoimprinting of the active material without breaking vacuum conditions during the device fabrication process.

High resolution e-beam lithography and inductively coupled plasma reactive ion etching were used to make a silicon mold having a square lattice pattern of circular holes. The diameter, depth, and pitch of the patterned holes were approximately 40, 90, and 100 nm, respectively. The size of the mold was ~1 $\times$ 1 in^2, and the size of the patterned area was 3 $\times$ 3 mm^2. In the imprinting step, ~5 mg of **5c** were heated just above its melting temperature (~70 °C) on a glass substrate (1 $\times$ 1 in^2). The mold was then pressed against the sample at a pressure less than 1 bar and held there until the sample cooled to ambient temperature. High mobility and low magnitude of wall slip at the melted sample/silicon interface enable us to directly imprint the nanostructures with high fidelity. After cooling, the glass substrate was released carefully from the mold without damaging the printed structure. A high resolution scanning electron microscopy image of nanopatterned **5c** (Figure 3b) shows nanostructures with an average diameter of 40 $\pm$ 5 nm and a height of 80−100 nm in a periodic array of cubic structures (with several squares of 0.5 mm $\times$ 0.5 mm area each). Cross-linking of the cinnamate residues by irradiating the surface with 300 nm light results in patterned nanostructures that are resistant to dissolution in chlorinated solvents (CH_2Cl_2, $CHCl_3$), which should allow subsequent wet processing steps to be performed. Figure 3c shows the SEM image of the nanostructures after cross-linking. (The image location on the nanostructure and imaging angle are not the same in Figure 3b and 3c.) The printed structures show high fidelity with the nanostructures of the silicon mold both before and after cross-linking. These nanopatterns can be printed in a few minutes and are highly reproducible.

Summary

In summary, we have demonstrated the modification of *Pc* chromophores with click chemistry and the subsequent use of installed functional groups to create robust cross-linked photopatterned and imprinted nanostructures. The investigation of these nanostructures as components of bulk heterojunction solar cells is currently underway in our laboratories.

Acknowledgment. This work was supported in part by the National Science Foundation (CHE-0719437) and by AZRise. Mold fabrication was done in the UCSB nanofabrication facility, part of the NSF funded NNIN network. We thank Neal Armstrong for helpful discussions, Mindy Horst for preliminary work, and Mayank Mayukh for synthesis of azides.

Supporting Information Available: Experimental details and additional characterization data for all new compounds. This material is available free of charge via the Internet at http://pubs.acs.org.

JA905683G